

INTERNATIONAL SOCIETY FOR SOIL MECHANICS AND GEOTECHNICAL ENGINEERING



This paper was downloaded from the Online Library of the International Society for Soil Mechanics and Geotechnical Engineering (ISSMGE). The library is available here:

<https://www.issmge.org/publications/online-library>

This is an open-access database that archives thousands of papers published under the Auspices of the ISSMGE and maintained by the Innovation and Development Committee of ISSMGE.

The paper was published in the proceedings of the 20th International Conference on Soil Mechanics and Geotechnical Engineering and was edited by Mizanur Rahman and Mark Jaksa. The conference was held from May 1st to May 5th 2022 in Sydney, Australia.

Buckling of micropiles in soft soil conditions – comparison of analytical approaches, FEM and real-scale in-situ pile loadtests

Flambage de micropieu dans des sols moux – comparaison des approches analytique, FEM et des essais in-situ échelle réelle de pieux

Patrick Ganne

Besix Engineering Department, Belgium, Patrick.ganne@besix.com

ABSTRACT: Micropiles are widely used as foundation piles. The steel elements (bars or small diameter tubes) transfer the vertical bearing loads down to the (compact) silt or sand layers. If the upper layers are soft (Holocene) peat and clay layers, the structural integrity of the micropiles is governed by the buckling failure mode. It is discussed that several analytical descriptions of the buckling phenomenon are inadequate for design considerations : the horizontal displacements of the micropiles and second order effects are to be taken into account. Furthermore, finite element analyses are too conservative if the soil-structure interaction is insufficiently detailed. It is demonstrated that low lateral soil support stabilizes the buckling micropiles in an important way. Therefore, it is concluded in buckling analyses to take into account : (1) the horizontal soil pressures at rest, and (2) the increasing horizontal soil pressures at lateral displacement of the micropiles.

RÉSUMÉ : Les micropieux sont utilisés comme pieux de fondation. Les éléments constructifs en acier transfèrent les efforts verticaux vers les sols silteux et sableux. Dans le cas des sols mous (tourbe et argile) superficiels, l'intégrité structurelle des micropieux est déterminée par le flambement. Il est montré que les descriptions analytiques sont trop limitées, parce qu'elles ne tiennent pas comptes des déformations horizontales et les effets de deuxième ordre. Par ailleurs, les analyses par éléments finis sont trop conservatrices si l'interaction sol-construction n'est pas simulée suffisamment en détail. Il est démontré que les efforts latéraux du sol stabilisent fortement le flambement des micropieux. Il est conclu qu'il faut prendre en compte : (1) pressions neutre comme efforts horizontaux par le sol, et (2) les efforts horizontaux, augmentant avec les déplacements latéraux des micropieux.

KEYWORDS: micropiles, buckling, soft soil, analytical approaches, FEM.

1 INTRODUCTION.

In accordance with the European standards (EN 14199), micropiles comprehend all piles with a diameter less than 300mm. In practice, micropiles are often 'small diameter' steel piles. The steel elements are mostly installed in different coupled pieces (of a few meters), after drilling the soil. The interaction between the steel pile and the surrounding soil, is created by injected grout.

Micropile technology has evolved significantly since its introduction in the 1950's. It took up to the 1980's when the use of micropiles increases successfully. Thanks to the small equipment and the ease of installation, micropiles are typically used for working under restricted access conditions : e.g. in zones that are in difficult way accessible for large pile rigs. They are typically applied for the underpinning of existing foundations, as tension piles for basement slabs, in extension of existing railway infrastructure...

The latest decennia, the use of micropiles evolves towards longer piles, higher bearing loads and softer soils. This evolution is driven by (1) the ease of making long piles by coupling steel parts of limited length together, (2) the good experience of behaviour of loaded micropiles, (3) the small equipment, accessing even very soft soil conditions. This evolution of long piles with small diameter, heavily loaded in soft soil environment, causes the buckling phenomenon governing in the design verification of compressive loaded micropiles.

BESIX, as part of the consortium 'De Groene Boog' realizes the highway connection between the A16 and the A13 at the north side of Rotterdam (Netherlands). This contract with the client RWS comprehends the design, build, finance and maintenance of this infrastructure. Among others, a bridge passing over the infrastructures of the high speed train has to be realized. Due to the length of these piles, this bridge is founded on micropiles. As the top layers are very soft clay and peat, the design of these micropiles is governed by its buckling behaviour.

Relating to the buckling behaviour of micropiles, the scientific background of buckling, the European execution codes, eurocodes, its national annexes and national guidelines are not coherent. This paper evaluates different methodologies to approach buckling, as well analytical approaches as different finite element evaluations. This evaluation is used on a real case study. The different approaches are evaluated by real-scale in-situ loadtests of the micropiles. Furthermore, a design approach is proposed and demonstrated.

2 BUCKLING OF MICROPILES : A COMPLEX SOIL-STRUCTURE INTERACTION

The analyses of flexural buckling of micropiles combines complex second order analyses of the structure with the strength-displacement soil behaviour.

2.2 Analytical approaches of buckling phenomena

The analytical description of flexural buckling of structures dates back to the Euler approach (1757). He describes that structures displace laterally when a critical normal load is exceeded. Based on the flexural stiffness EI and the length of the structure, the equilibrium of moments results in the Euler differential equation. The analytical solutions of the Euler buckling force is well known:

$$N_{buc} = n^2(\pi/L)^2 EI \quad (1)$$

n the buckling mode $n = 1, 2, 3, \dots$

L the length of the structure [m]

EI the flexural stiffness of the structure [Nm²]

The critical buckling force at wavenumber $n = 1$

This description is based on hinged ends assumption; the clamped ends solutions are available in literature. In these analytical solutions is assumed that the structure is laterally unsupported.

Engesser (1884) extends the Euler buckling approach for structures with lateral support. The support is mathematically

introduced as linear elastic springs. This results in the buckling formulation for piles (Bjerrum, 1957):

$$N_{buc} = n^2(\pi/L)^2 EI + (L/n\pi)^2 k \quad (2)$$

k the modulus of lateral reaction of the soil [N/m²]

The critical buckling force at wavenumber $n = 1$

Vogt et al. (2005 and 2006) elaborates this analytical approach, introducing a linear elastic, perfect plastic spring as lateral support and an initial imperfection of the pile.

For the critical buckling force N_{cr} [N]:

$$N_{cr} = \frac{y_{ki} \left(\frac{\pi}{L_{cr}} \right)^2 EI + k y_{ki} \left(\frac{L_{cr}}{\pi} \right)^2}{y_{ki} + w_0} \quad (3)$$

y_{ki} maximal elastic deformation of soil [m]
 w_0 initial deformation of the pile [m]
 L_{cr} the critical buckling length [m]

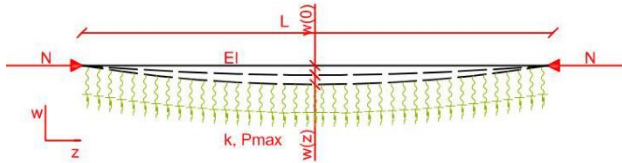


Figure 1. Schematisation of buckling analyses as by Vogt (in Lankreijer, 2014).

Lankreijer (2014) combines the Vogt and Eurocode (EN1993-1-1) solution, to obtain the buckling resistance of micropiles as the sum of three components:

$$N_{cr,pile} = (N_{cr,steel} + N_{cr,grout} + N_{cr,soil}) \quad (4)$$

(1) contribution of steel resistance is based on EN1993-1-1 :

$$N_{cr,steel} = \chi f_y A_{steel} \quad (4a)$$

(2) contribution of the surrounding grout

$$\frac{1}{N_{cr,grout}} = \frac{\xi}{EI_g \frac{y_{ki}}{y_{ki} + w_0} \left(\frac{\pi}{L_{cr}} \right)^2} + \frac{\xi}{f_{cd} A_g} \quad (4b)$$

(3) contribution of surrounding soil support.

$$N_{cr,soil} = \frac{k y_{ki} \left(\frac{L_{cr}}{\pi} \right)^2}{y_{ki} + w_0} \quad (4c)$$

χ reduction factor buckling curve (EN1993-1-1)

f_y, f_{cd} yield strength for steel and grout

A_{steel}, A_g surface of steel and grout

ξ reduction factor for amount of contribution of grout

EI_g flexural stiffness of grout

Introducing the reduction factor χ , the influence of relative slenderness, the class of steel section and the imperfection factor (hot rolled or cold formed) is introduced.

2.2 Buckling of micropiles in soft soils

In the Vogt and Lankreijer approach of buckling, the soil is represented as a linear elastic, perfect plastic spring. As the normal force increases and approaches the critical buckling force, the lateral deformation of the pile engenders an increase of the lateral support by the soil, limited to a maximum (p_{100} [N/m]):

$$p_{100} = y_{ki} \cdot k \quad (5)$$

For undrained clay soil, Brinch-Hansen (1961) describes the maximum soil support at the maximum soil pressure, as:

$$p_{100} = N_c c_u D \quad (6)$$

c_u the undrained cohesion [N/m²]
 D the diameter of the pile [m]

N_c the factor for maximum soil pressure : between 9.14 and 11.9, depending of the roughness of the pile. Reese et al. (2001) determines the lateral deformation of clays at horizontal loaded piles, as $y = 2.5 e D$. The maximum soil support (p_{100}) is reached at a lateral displacement (y_{ki}) of 10% of the pile diameter ($e_{100} = 0.04$). Defining the linear modulus of lateral reaction of the soil (k), as secant stiffness (k_{50}) at 50% of the maximum soil support:

$$k = k_{50} = 90 c_u \quad (7)$$

At most micropiles, grout surrounds the steel elements. As the grout is much stiffer than the surrounding soft soil, the maximum soil support is engendered by the lateral displacement of the steel and grout parts as a whole. In this reasoning, the diameter of the pile D has to be taken as the diameter of the grout.

Remark that in the Engesser formulation, the buckling force is determined by the wave number. The critical buckling force is the minimum buckling force at all wave numbers ($n = 1, 2, 3, \dots$). For a micropile surrounded by soil, all buckling modes are possible, as long as its critical length is smaller than the thickness of the soft soil layer:

$$L_{cr} \approx a \sqrt[4]{4EI/k} \quad (8)$$

and $L_{cr} < \text{thickness of the soft soil layer}$

$a = p$ (theory of Engesser)

$a = 5$ (Verruijt, 2006)

Caused by the typical low flexural stiffness of micropiles, the critical buckling length may become as small as a few meters. This suggests that buckling could govern the structural design when micropiles transfer soft layers as small as a few meters.

3 CASE STUDY : MICROPILES AS FOUNDATION OF A BRIDGE AT ROTTERDAM

For the highway connection between the A16 and the A13 at the north side of Rotterdam (Netherlands), a bridge (K22b) passing over the infrastructure of the high speed train has to be realized. The width of the box girder bridge amounts to about 50m. The span of the bridge is about 35m. The abutments are founded on three rows of micropiles.

3.1 Local soil conditions

The soil consists out of Holocene soft clay and peat up to 12m below soil level, with underneath dense sand layers. At 31m below ground level, the soft 'clay of Kedichem' is encountered. Over a depth of 16 meters soft clay of Kedichem is alternated by silty sand layers.

Table 1. Overview of geotechnical soil layers with typical results of eCPT (electronic cone penetration tests).

Meters below soil level	Soil type	q_c [MPa]	r_f [%]
0 – 12m	Soft clay and peat	0.1 – 0.5	2 - 8
12m – 31m	Dense sand	15 – 25	1
31m – 47m	Alternation clay of Kedichem	3	4
	silty sand	4 – 15	1 - 2
Below 47m	Very dense sand	25 - >50	1

Table 2. Typical drained and undrained characteristic strength properties of the encountered soft clay and peat (Holocene between 0m and 12m below soil level).

Soil	Saturated density [kN/m ³]	f' [°]	c' [kPa]	C_u [kPa]
Peat H	10 – 11	15	2.5	10
Peat B	11 – 12	17.5	3.0	10
Clay silty	14.5 – 16.5	22.5	6.5	10
Clay sandy	> 16.5	26	4.0	10

Table 3. Typical stiffness parameters (Plaxis input for hardening soil elements) of the encountered soft clay and peat (Holocene between 0m and 12m below soil level).

Soil	E_{oed}^{ref} kN/m ²	E_{ur}^{ref} kN/m ²	OCR	m	Pref kPa
Peat H	510	4000	2.0	0.9	100
Peat B	800	6400	2.0	0.9	100
Clay silty	1500	12000	1.6	0.9	100
Clay sandy	2750	22000	1.6	0.9	100

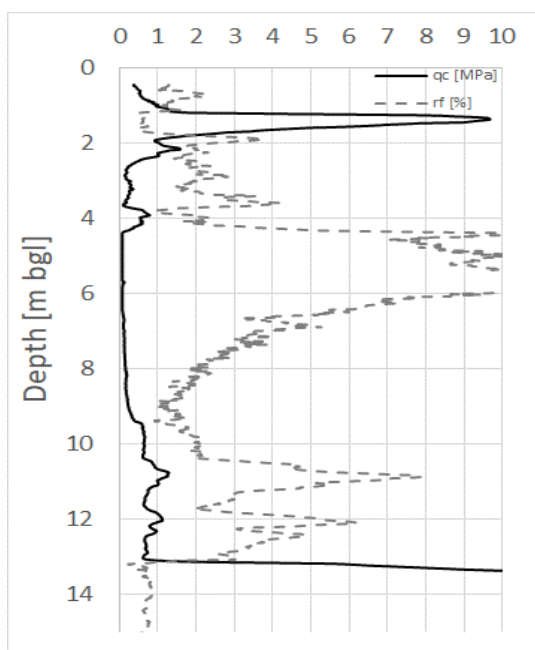


Figure 2. Typical result of electric cone penetration test at abutments of bridge K22b over the soft holocene layers : cone resistance (q_c [MPa]) and sleeve resistance (r_f [%]).

3.2 Installation of micropiles at k22b

In these soil types, the micropiles are installed according to the 'self-drilled' procedure and a lost drill head. These micropiles consists of a self-drilling hollow steel bars of 3 meters length,

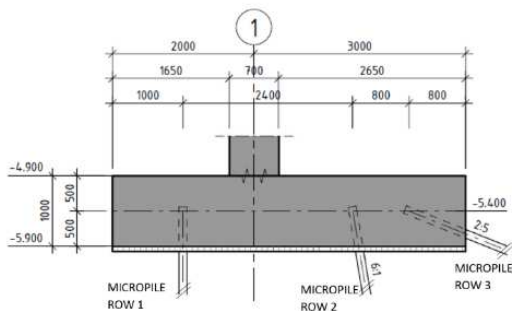
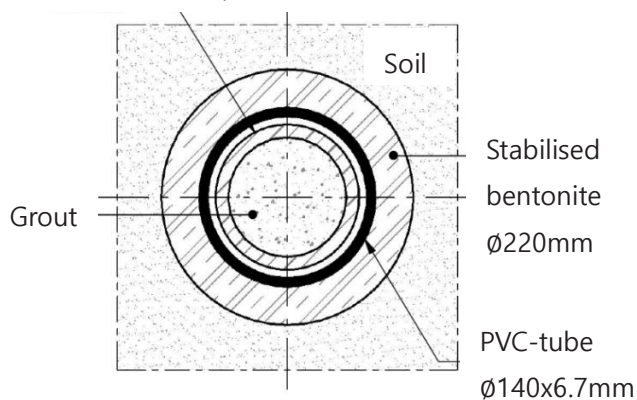


Figure 3. Typical cross section of the foundation part of the abutment at axis 1 of K22b, measures are in mm, the micropiles are not in real lengths.

Hollow steel bar $\varnothing 114 \times 10$ mm



Hollow steel bar $\varnothing 114 \times 10$

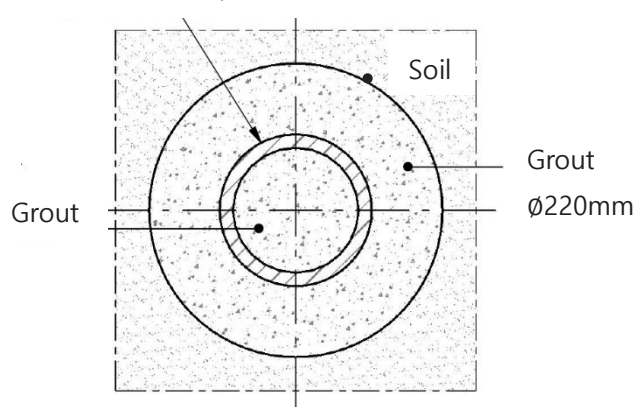


Figure 4. Schematic cross section of the micropile over the free length (upper) and groutlength (lower).

coupled together by internal thread. The hollow steel bars have a diameter of 114 mm and a thickness of 10 mm (steel quality N80, $f_y = 560$ MPa). During the drilling process, a drilling fluid of poor water-cement is used. As the base level is reached, the drilling fluid is replaced. Along the grouting length, these hollow bars are embedded within a grout body of diameter of 220 mm. Along the free length, these hollow bars are embedded in cement stabilized bentonite and a gliding PVC-tube (diameter of 140 mm).

The micropiles of rows 1 and 2 are loaded up to 500 kN (SLS) compression (700 kN ULS). The third row of micropiles maintains the horizontal forces and limit the horizontal displacement of the abutment. These micropiles are installed sub-horizontal and mainly loaded by tensile forces (< 350 kN). For reasons of reduction of settlements of the nearby high speed train infrastructure, the micropiles of row 1 have to transfer the loads to the deeper sand layers, underneath the soft 'clay of Kedichem'. Therefore, the transfer of the pile loads to the surrounding sand start at 46 m below soil surface. These 46 m have to be installed as 'free length micropile'. As the designed groutlength is 13 m, the total length of the installed micropiles of row 1 amounts to 59 m.

Table 4. Overview of the installed micropiles, length and load.

Micropile	Inclination	Free length	Total length	Maximum load (SLS)
Row 1	Vertical	46 m	59 m	500 kN (compression)
Row 2	Sub-vertical 6/1	12 m	25 m	500 kN (compression)

Row 3	Sub-horizontal 2/5	32m	48m	350kN (tension)
-------	-----------------------	-----	-----	--------------------

Table 5. Overview of the number of installed micropiles and the minimum distance in between.

Micropile	Abutment axes 1	Abutment axes 2	Minimal interdistance hart-on-hart
Row 1	102	102	0.75m
Row 2	192	192	0.75m
Row 3	33	33	2.25m

3.3 Evaluation of buckling of micropiles at abutment of k22b

Micropiles of row 1 and row 2 are installed to great depths. Over the first 12m, soft clay and peat is present, causing the buckling resistance to be the governing structural failure mode of the micropiles. Furthermore, over these soft soil layers, the micropiles are installed as ‘free length’: the transition of normal loads to the surrounding soil is minimized, bentonite and gliding PVC tube surround the steel bars. At the other hand, the lateral soil support is necessary to prevent buckling: without soil support, the critical buckling force is about 5kN (Euler: $EI = 968\text{kNm}^2$; $L = 46\text{m}$) for micropiles at row 1. Even for micropiles at row 2, with a free length of 12m, the critical buckling force is 65kN (Euler: $EI = 968\text{kNm}^2$; $L = 12\text{m}$), far from the 500kN bearing load. In order to maintain the lateral soil support, the bentonite is stabilized by addition of cement (300kg/m^3). The stabilized bentonite is stiffer and has higher strength (0.5N/mm^2) than the surrounding soft clay and peat, which maintains the stabilizing lateral soil support.

Vogt (2) takes the lateral soil support into account. The maximum soil support of $p_{100} = 18\text{kN}$ (6) per meter of micropile is obtained at a lateral displacement of $y_{ki} = 0.02\text{m}$, corresponding to a modulus of lateral reaction of the soil $k = 900\text{kN/m}^2$. The initial deformation of the pile at installation, is based on the values of EN14199: a curve radius of 200m, corresponding to an installation deviation of 0.0018m per meter depth. The critical buckling length is 2.75m, obtaining an initial deformation of pile $w_0 = 50\text{mm}$. Hence, the critical buckling force, using Vogt’s formulation, amounts to 1084kN (3).

With the same assumptions, the critical buckling force, using Lankreijers formulation (4), amounts to 973kN. The differences between both results is within 10%. On the other hand, Lankreijer (2014), based on EEM evaluations, advises to reduce the modulus of lateral reaction of the soil (8) to

$$k = 65 \text{ Cu} \quad (9)$$

and advises to consider that the maximum lateral soil support is reached at a lateral displacement y_{ki} of 5% of the pile diameter ($e_{100} = 0.02$ in Reese et al., 2001). Both assumptions reduces the critical buckling force further to 797kN (i.e. reduction of 20%).

As the soil-structure interaction is significant in the determination of the buckling force of micropiles, 3D finite element evaluation (Plaxis 3D v.20.0.1.128) is used to evaluate the interaction of the 0.20m diameter micropiles with the soft holocene soil at K22b (table 3). A single micropile is modelled within a 20 by 20m soil model and 5m depth. In total, 29000 3D volume-elements are used. The soil is modelled with hardening soil elements, the input properties are ‘clay, silty’ in table 3. The micropile is modelled by linear elastic volume-elements: $E = 8.4 \cdot 10^6\text{kN/m}^2$, coefficient of Poisson $\nu = 0.25$. A horizontal line load along the depth of the micropile is applied for increasing load steps from 1 to 18kN/m. At a horizontal line load of 4kN/m along the micropile, the calculated horizontal displacements of the micropile varies between 2.8 (at surface) and 1.2mm (at 5m depth, figure 5). The horizontal displacements are limited as long the horizontal line load does not exceed the initial horizontal soil pressure. These initial horizontal soil pressure increases from 0kPa (at surface) to about 12.5kPa at 5m depth. For the 0.2m diameter micropile, this corresponds to a horizontal initial

stabilising load up to 2.5kN (at 5m depth). Figure 6 gives the corresponding calculated maximum horizontal displacements of the modelled micropile at different horizontal line load steps. It demonstrates that in the present case study, the Brinch-Hansen/Reese assumptions (6, 7) overestimates the lateral soil support when lateral displacements increases 10mm. The reduction of Lankreijer underestimates the lateral soil support. At small displacements, both Hansen/Reese and Lankreijer underestimates the lateral soil support. At a lateral displacement of 2.8mm, the soil support is 4kN/m and the modulus of lateral reaction of the soil amounts to 1400kN/m^2 .

This soil-structure interaction is introduced in a structural finite element (SciaEngineer v.18.1.3035) model. A micropile is simulated by a beam with $EI = 968\text{kNm}^2$ of 12m length, inclusive an initial curvature of $R = 200\text{m}$. The beam is hinged at the toe. The lateral soil support is simulated by springs with modulus $k = 1400\text{kN/m}^2$. The introduced normal load of the micropile is 689kN. Figure 7 suggests that the calculated lateral displacements do not exceed 2.8mm and the lateral soil support does not exceed 4kN/m, indicating the validity of the modulus $k = 1400\text{kN/m}^2$. The calculated $a_{crit} = 1.70$, resulting in a calculated Euler buckling force of $689 \cdot 1.70 = 1171\text{kN}$ (EN1993-1-1).

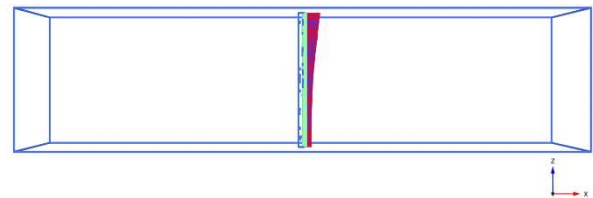


Figure 5. FEM (Plaxis) 3D – calculated horizontal displacements of the micropile with 4kN/m horizontal line load.

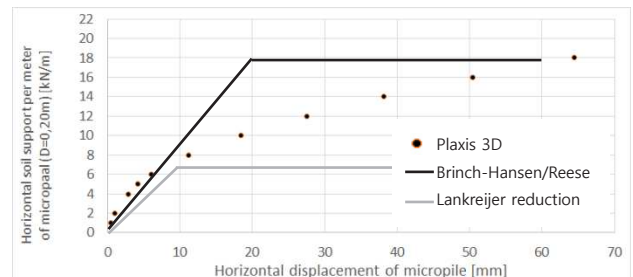


Figure 6. FEM (Plaxis) 3D determination of the horizontal soil support per meter of micropile (diameter = 0.20m) [kN per meter of micropile] at various horizontal displacements of micropile [mm]. The Brinch-Hansen/Reese (6), (7) assumptions and the reduction as suggested by Lankreijer are correspondingly indicated in black and grey lines.

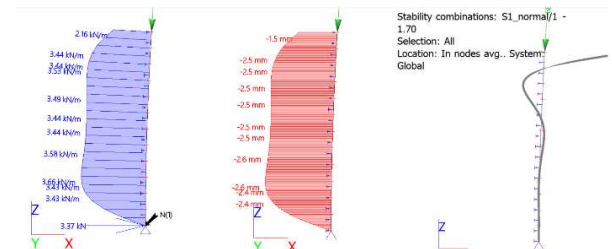


Figure 7. FEM (SciaEngineer) results at normal load of 689kN: lateral soil support (left), lateral displacement (mid) and buckling mode (right).

All buckling approaches, based on linear elastic springs, neglect the complicated non-linear soil-micropile interaction. In a continuum finite element simulation (Plaxis 2D), micropiles are

simulated by 'embedded beams' type 'elastic' with a surface, stiffness and flexural rigidity of the steel bar. The spacing amounts to 0.75m. The lateral stiffness factor is increased up to 25, in order to take 3D effects into account. The value is based on the simulated micropile-soil interaction as by previously described Plaxis 3D. Installation tolerances are simulated by an initial curvature of the micropile of $R = 200\text{m}$. All Holocene soft soils and 10 meters of dense underlying sand are modelled (table 1) with 'hardening soil' elements. The horizontal extent of the model amounts to 30m, in plain strain mode. In total 8500 elements are modelled. The vertical load on the micropile is increased by loading steps. At higher load, the simulation become unstable, indicating a critical buckling load of 1690kN. The critical buckling length is not a outcome of the Plaxis simulation, though, the lateral displacements of the micropile are very similar. The soil-micropile interaction simulated by the continuum finite element code (Plaxis), results in higher lateral soil support at small lateral deviation of the micropile. Even without lateral displacement of the micropile, the soil support is significant : the horizontal soil pressure 'at rest'. In the case of a 0.2m diameter micropile, in the silty clay ($g = 15\text{kN/m}^3$, $K_0 = 0.61$); this lateral support amounts to a mean value at the first meter of about 1 to 2kN. This amount of lateral support of the soil at rest, stabilises the buckling of the micropile significantly.

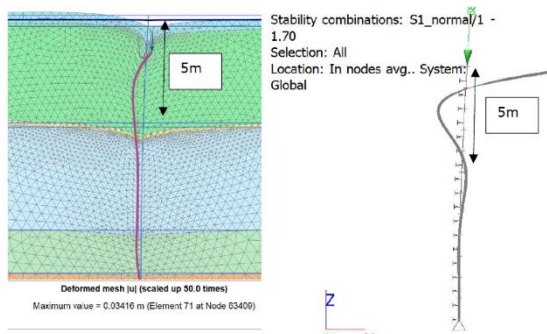


Figure 8. Results of displacements of a micropile in a continuum FEM (Plaxis 2D) at 1500kN (left) compared to the buckling mode as calculated by FEM (SciaEngineer) (right).

3.4 Pile tests

The critical buckling force of a micropile in soft soil, is demonstrated to be significantly higher than the unsupported Euler buckling force (i.e. 5kN) : 1355kN (Vogt, 3) and 1084kN (Lankreijer, 4). Taking the installation tolerance of curvature $R = 200\text{m}$, into account, the critical buckling force amounts to:

- 1084kN (Vogt, 3)
- 797kN (Lankreijer, 4)
- 1171kN (Scia Engineer)
- 1690kN (Plaxis 2D)

The micropiles of the foundation of K22B are designed for loads up to 500kN (SLS) compression (700kN ULS). Two in-situ real-scale load test demonstrate (1) the presence of the lateral soil support in the free length and (2) the stabilizing influence of the soil support on the critical buckling force.

Two micropiles, P1 and P9, are installed nearby the location of the western abutment of K22B by self-drilled procedure. These micropiles are 67m deep, including a free length of 48m (figure 4) through the soft holocene soil, the dense sand and the clay of Kedichem (table 1). The micropiles are grouted using a water-cement ratio of 0.5; the cement type is CEM III/B 42.5. The grouting continues until the grout is visually observed at ground level, leading to a theoretical overconsumption of 20% of the grout. Along the free length, stabilized bentonite is injected throughout the annular space between the PVC-tube and the steel bar. At the base level of the PVC-tube, the stabilized bentonite is coming upwards at the outside of the PVC-tube up to the soil

level. Hence, the grout is replaced along the free length at the annular space between the PVC-tube and the steel bar, as well as the outside of the PVC-tube. At micropile P1, the injection of the stabilized bentonite is continued until its visual observation at ground level. At micropile P9, no visual observation of the stabilized bentonite is reported at ground level, even after a theoretical overconsumption of 93%. Therefore, it is concluded that for micropile P9, the stabilized bentonite has replaced the grout at the annular space between the PVC-tube and the steel bar; it cannot be concluded that the grout at the outside of the PVC-tube is replaced along the total free length. The stabilized bentonite consists out of 300kg/m^3 cement (CEM III/B 42.5) and 30kg/m^3 of bentonite; resulting in a uniaxial strength exceeding 500kPa after 28 days. A pile head of diameter 500mm and height of 0.5m is poored with concrete. The pile head is isolated from the underlying soil by soft isolation, to limit the transfer of forces directly to the soil and to maximise the transfer of the loading to the micropile.

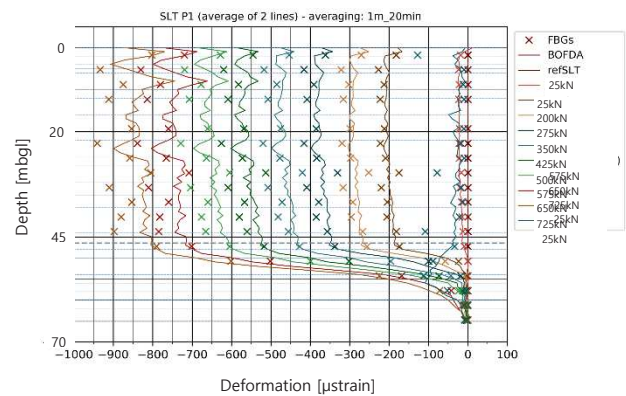
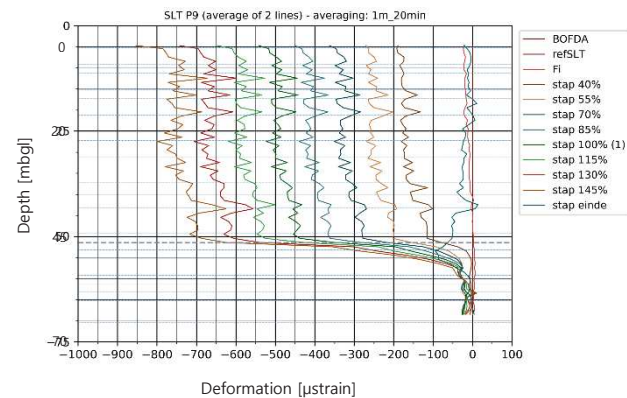


Figure 9. Monitored axial deformation of loaded micropiles P1 (upper)



and P9 (lower) during the in-situ real-scale load test.

Both micropiles are equipped with optical fibre type 'BOFDA' (Brillouin optical frequency domain analysis, measure precision of 10 microstrain, one measure each 300 seconds). Micropile P1 is additionally equipped by optical fibre type 'FBG' (Fibre bragg grating, measure precision of 1 microstrain, one measure each 10 seconds). Both micropiles are loaded up to 725kN : starting at 25kN, the load is increased to the loadlevel of 200kN, 275kN, 350kN, 425kN and 500kN at a rate of 75kN/hr. Each load level is maintained for 1hr. The 500kN load level is maintained for 12hr, whereafter the load is further increased up to 575kN, 650kN and 725kN. Also these loadlevels are maintained for 1hr. The load is controlled by a 1490kN load cell and monitored by a calibrated dynamometer (accuracy of 1kN). The reaction system consists out of two water-filled containers, with a total weight of 90ton. The displacements of the pilehead

is measured by 4 electronic LVDT Solarton (measure precision of 0.01mm), and verified by a total station system.

The monitoring of the deformation along the micropiles, indicates a limited reduction of axial deformation along the free length (figure 9). Considering the axial stiffness of the micropile, the force reduction along the 48m free length is calculated (figure 10) : at a service load of 500kN, the axial load of the micropile is reduced by 80kN (P1) and 18kN (P9) along the 48m free length. This suggests that in average, less than 1.7kN per meter of free length, is transferred to the surrounding soil. This is considered as an appropriate behaviour of a good working 'free length'. Though, no buckling of the micropile during the 725kN load test has occurred. As the critical buckling load of the unsupported micropile amounts to 5kN, the absence of buckling suggests that lateral soil support is present along the free length.

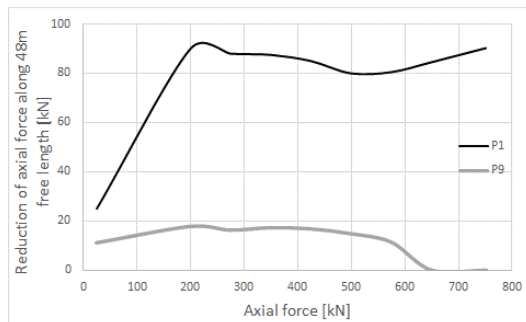


Figure 10. Reduction of axial force [kN] along 48m of free length in function of the applied axial load [kN] during loadtests of micropiles P1 and P9.

4 DESIGN CONSIDERATIONS

EN14199-2005 indicates that a check for buckling is required for micropiles installed through soil layers with characteristic undrained strength of less than 10kPa. It is the author's experience that even in soil layers with characteristic undrained strength of above 10kPa, buckling may be governing in design.

The structural design of micropiles has to take the buckling into account. For instance, in EN 1993-1-1, the buckling resistance is based on a reduction of the elastic buckling load (Euler load) by the reduction factor c : taking into account the cross-section shape, the process of fabrication (such as cold formed or hot finished), yield strength and imperfection factor. Implicitly, an initial tolerance is used, and, hence an internal bending moment is taken into account as 'second order moment'. The lateral support of the surrounding soil is a significant stabilizing factor. As a consequence, the critical buckling length of micropiles is reduced to typically a few meters. Furthermore, as even low lateral support stabilizes the buckling, it is significant to simulate correctly the soil-structure interaction at low horizontal displacements :

- stiff soil-structure interaction at low lateral displacements
- lateral soil support with no lateral displacement (soil at rest)

In general ($a_{crit} < 10$), a second order buckling analyses will be necessary. It is significant to explicitly consider the initial tolerances : the installation tolerance of the micropile. EN14199 suggests a radius of curvature of 200m as the installation tolerance. Alternatively, a maximum angle of deviation in the micropile joints of 1/150 radian can be considered. Lankreijer (2014) suggests that using larger casings during the drilling procedure (instead of small diameter bars, typical for self drilling micropiles), the installation tolerance can be as less as $w_0 = L/900$. It is obvious that the installation tolerance should be evaluated based on the drilling procedure (large or small diameter drill casing), the local heterogeneity of the soil, the

number of joints and so forth. At the other hand, the horizontal displacements of the abutments, will additionally cause horizontal deformations and additional moments of the micropiles. For instance the case of K22b, 20mm horizontal displacement of the abutments is calculated. Therefore, the head of the micropiles will also displace horizontally and a destabilising moment of 4kNm per micropile is determined. This amounts to almost 10% of the moment capacity of the micropile. These destabilising effects are to be taken into account in the stability verification.

5 CONCLUSIONS

Micropiles are used as axially loaded foundation piles for civil constructions. Due to the small diameter of micropiles, lateral soil support is necessary for the structural buckling stability. In sandy soils, the lateral soil support is generally sufficient, and an explicit buckling verification is expected to be not governing. In soft soil conditions, even if the soft layer is as thin as one or two meter, buckling may become governing. It is demonstrated that, contrary to the EN14199, buckling may become governing in the case of undrained strength above 10 kPa.

The lateral soil support is significant in the determination of the buckling stability of micropiles. The analyses of buckling of micropiles combines complex second order analyses of the structure with the strength-displacement soil behaviour. The small lateral soil support at low lateral displacements are very significant. Therefore, the stiff soil-structure interaction at low displacements and the lateral soil support at rest (without lateral displacement) have to be adequately considered.

In general ($a_{crit} < 10$), a second order buckling analyses will be necessary in the structural design. The structural verification of the micropiles are governed by the presence of installation tolerances and horizontal displacements during serviceability. Therefore, the analytical approaches of Engesser (2), Vogt (3) and Lankreijer (4) are not adequately covering a full design verification. FEM, including the simulate of the complex soil-structure interaction and including the complex second order analysis of buckling, are necessary for appropriate design verifications.

6 REFERENCES

- Bjerrum L. 1957. Norwegian experiences with steel piles to rock. *Geotechnique* 7, 73-96.
- Brinch-Hansen J. N.H. 1961. The ultimate resistance of rigid piles against transversal forces. The Danish Geotechnical Institute, Bulletin 12, 1-9.
- Cadden A. P.E. and Gómez J.P.D. 2002. Buckling of micropiles – A review of historic research and recent experiences. ADSC-IAF – Micropile Committee.
- CUR Bouw & Infra. 2011. CUR236 : Ankerpalen. CURNET.
- EN 14199. 2015. Execution of special geotechnical works – micropiles. CEN/CENELEC
- EN 1993-1-1. 2005. Design of steel structures – Part 1-1 : General rules and rules for buildings. CEN/CENELEC
- Lankreijer T. 2014. Buigingsknik van ankerpalen – staal, grout en grond. Msc Thesis. TUDelft. Delft.
- Reese L.C., Impe Van W.F. 2001. Single pile and pile group under lateral loading. Balkema, Rotterdam.
- Shields D.R. 2007. Buckling of micropiles. *Journal of Geotechnical and Geoenvironmental Engineering* 133(3), 334-337
- Vogt S., Vogt N. and Kellner C. 2005. Knicken von Pfählen mit kleinem Durchmesser in breiigen Böden. Technische Universität München : Deutsches Institut für Bautechnik. München.
- Vogt S., Vogt N. and Kellner C. 2006. Knicken von schlanken Pfählen. Verruijt A. 2006. Offshore soil mechanics. TUDelft. Delft.
- Youssef E. 1994. Etude théorique et expérimentale du flambement des pieux. Matériaux. Msc thesis. Ecole Nationale des Ponts et Chaussées. Paris.